Chemical Force Spectroscopy in Heterogeneous Systems: Intermolecular Interactions Involving Epoxy Polymer, Mixed Monolayers, and Polar Solvents

Dmitri V. Vezenov,*,† Andrew V. Zhuk,‡ George M. Whitesides,† and Charles M. Lieber†

Contribution from the Department of Chemistry and Chemical Biology and Division of Applied Sciences and Engineering, Harvard University, Cambridge, Massachusetts 02138

Abstract: We used chemical force microscopy (CFM) to study adhesive forces between surfaces of epoxy resin and self-assembled monolayers (SAMs) capable of hydrogen bonding to different extents. The influence of the liquid medium in which the experiments were carried out was also examined systematically. The molecular character of the tip, polymer, and liquid all influenced the adhesion. Complementary macroscopic contact angle measurements were used to assist in the quantitative interpretation of the CFM data. A direct correlation between surface free energy and adhesion forces was observed in mixed alcohol−water solvents. An increase in surface energy from 2 to 50 mJ/m^2 resulted in an increase in adhesion from 4−8 nN to 150−300 nN for tips with radii of 50−150 nm. The interfacial surface energy for identical nonpolar surface groups of SAMs was found not to exceed 2 mJ/m^2. An analysis of adhesion data suggests that the solvent was fully excluded from the zone of contact between functional groups on the tip and sample. With a nonpolar SAM, the force of adhesion increased monotonically in mixed solvents of higher water content; whereas, with a polar SAM (one having a hydrogen bonding component), higher water content led to decreased adhesion. The intermolecular force components theory was used for the interpretation of adhesion force measurements in polar solvents. Competition between hydrogen bonding within the solvent and hydrogen bonding of surface groups and the solvent was shown to provide the main contribution to adhesion forces. We demonstrate how the trends in the magnitude of the adhesion forces for chemically heterogeneous systems (solvents and surfaces) measured with CFM can be quantitatively rationalized using the surface tension components approach. For epoxy polymer, inelastic deformations also contributed heavily to measured adhesion forces.

Introduction

Interfaces designed at the molecular level provide an opportunity to study intermolecular forces between dissimilar materials. Amorphous interfaces involving organic materials are present in problems of both industrial and academic interest, for example, compatibility of polymer phases, lubrication, adsorption, biological adhesion, or susceptibility of interfaces to changes in environmental conditions.[1,2] In many engineering, chemical, or biological processes, the behavior of these interfaces reflects the combined response of the system as a whole to external stress. For example, the observed interfacial strength will be influenced by the strength of the intermolecular interactions at the interface, the mechanical properties of the bulk material (plastic and viscoelastic contributions), and the rates of stress application (temperature and velocity dependencies). Forces and energies involved in the breaking of adhesive joints (fracture energies) are typically orders of magnitude higher than estimates based on the thermodynamic work of adhesion.[3] Methods that disentangle intermolecular forces from other factors (e.g. viscoelastic dissipation of energy) are extremely valuable. In the present work, we attempt direct experimental measurements of the intermolecular component in the overall strength.

Typically, intermolecular surface forces are interpreted in terms of basic interactions such as van der Waals, electron donor−acceptor (hydrogen bonding), and electrochemical interactions.[1] Most experimental data on the thermodynamics at the interfaces come from studies of surface or interfacial tension and wettability,[4−11] adsorption and immersion calorimetry,[4,5,12−14]

---

* To whom correspondence should be addressed. Current address: Calimetrics, Inc., 19 Crosby Dr., Suite 130, Bedford, MA 01760. E-mail: dvezenov@calimetrics.com.

† Department of Chemistry and Chemical Biology.

‡ Division of Applied Sciences and Engineering.

(1) Israelachvili, J. *Intermolecular and Surface Forces*; Academic Press: New York, 1992.
(2) Bhushan, B. *Handbook of Micro/Nano Tribology*, 1st ed.; CRC Press: Boca Raton, FL, 1995.
(3) Evans, A. G.; Dalgleish, B. J. *Acta Metall. Mater.* **1992**, *40*, S295.
(4) Fowkes, F. M. *Ind. Eng. Chem.* **1964**, *56*, 40.
(5) Fowkes, F. M. In *Surfaces and Interfaces I. Chemical and Physical Characteristics*; Burke, J. J., Reed, N. L., Weiss, V., Eds.; Syracuse University Press: Syracuse, NY, 1967; p 197.
(6) Good, R. *J. Colloid Interface Sci.* **1977**, *59*, 398.
(7) Van Oss, C. J.; Chaudhury, M. K.; Good, R. J. *Chem. Rev.* **1988**, *88*, 927.
(8) van Oss, C. J.; Good, R. J.; Chaudhury, M. K. *Langmuir* **1988**, *4*, 884.
(9) Janczuk, B.; Wojcik, W.; Zdziennicka, A. *J. Colloid Interface Sci.* **1993**, *157*, 384.

reversed phase chromatography,[15] and inverse gas chromatography.[16,17] A direct method of estimating the work of adhesion based on contact mechanics was developed by Chaudhury.[18] This method measures the deformation produced on contacting elastic hemispheres under the influence of surface forces and external loads. The method is macroscopic and limited to elastic transparent materials and low interaction energies. Adhesion between homogeneous molecular assemblies adsorbed on a molecularly smooth probe and sample areas has been studied with the surface force apparatus[19,20] but provides data averaged over a macroscopic area ($\sim$1 mm^2). Measurements of the noncontact forces due to van der Waals,[21,22] acid–base,[23] and electrostatic interactions[24–27] between a micrometer size probe and flat substrates have been carried out using a colloidal probe microscope.

In the work described here, we pursue another attractive option and use an atomic force microscope (AFM) with sharp probes.[28] Intermolecular interactions can then be probed in the dynamic mode using force measurements at truly nanoscopic scale (between tens or hundreds of molecules). Sample requirements for these types of experiments are significantly more relaxed than those for experiments requiring large, flat, ordered areas of sample.

The development of a fundamental understanding of intermolecular interactions at organic interfaces can be achieved by designing the interfaces and/or intervening medium in such a way that the strength and type of interaction can be systematically varied. We attain this objective with a systematic force microscopy study of interactions between molecular groups based on a concept of chemical force microscopy (CFM) that exploits specifically functionalized AFM tips to study intermolecular interactions on a nanometer scale.[29–31] With this approach, the chemical identity and surface energy of the probe is controlled by covalently linking a self-assembled monolayer (SAM) terminating in a distinct functional group to the tip surface. Force measurements can be conducted in a liquid medium, and, hence, solvent chemical effects on the interaction between organic group assemblies can be analyzed. Combining these features with unique sensitivity (sub-nanonewton) and

resolution (sub-nanometer) of the AFM, yields a technique capable of providing information about intermolecular interactions at nanometer scale.[32–40] Recent success in chemical mapping of the surface functionality of oxidized polymer films with sub-50 nm resolution using CFM[41] points to the need to move to more complex, chemically heterogeneous systems, such as polymers, mixed monolayers, and solvents to advance the fundamental aspects of the chemical force microscopy.

Force spectroscopy data in CFM experiments have typically been interpreted by employing the contact mechanics to describe tip–sample interactions. The prediction of the contact mechanics that the adhesion force scales proportionally with the tip radius of curvature has been convincingly shown to hold for pull-off measurements at nanometer scale.[42] In this work we demonstrate in a systematic way that pull-off forces determined with CFM also scale directly with the work of adhesion, as expected from the contact mechanics, and investigate conditions under which this relationship is not valid. Since typical CFM experiments are performed under a liquid medium, we address the role of the solvent in detail and demonstrate that solvent–solvent interactions are an integral part of the measured force of adhesion in chemical force spectroscopy and must be appreciated especially when hydrogen bonding interactions are present.

Interaction forces in heterogeneous systems are beginning to be probed with CFM, polymers being one application of high interest.[41,43–46] In previous force spectroscopy work on polymers in an apolar solvent using predetermined probe chemistry (plasma treated oxidized silicon nitride and gold coated tips),[46] polymers of various composition could be distinguished on the basis of the measured adhesion. This differentiation enabled imaging of polymer blends with chemical sensitivity and predictable chemical contrast. The force values were generally found in agreement with theoretical calculations of Hamaker constants but deviated from theory in cases when hydrogen bonds could form between tip and sample functional groups. We attempted chemical force spectroscopy experiments using a polymer in a heterogeneous system where all components (polymer surface, probe, and solvent) are capable of hydrogen bonding. We systematically varied the extent of hydrogen bonding and used the framework developed for the interpretation of CFM adhesion data in polar solvents to address the applicability of contact mechanics to CFM studies of polymers.

(10) Correia, N. T.; Ramos, J. J. M.; Saramago, B. J. V.; Calado, J. C. G. *J. Colloid Interface Sci.* **1997**, *189*, 361.
(11) Lee, L.-H. *Langmuir* **1996**, *12*, 1681.
(12) Douillard, J. M.; Elwafir, M.; Partyka, S. *J. Colloid Interface Sci.* **1994**, *164*, 238.
(13) Douillard, J. M. *J. Colloid Interface Sci.* **1997**, *188*, 511.
(14) Janchen, J.; Stach, H.; Uytterhoeven, L.; Mortier, W. J. *J. Phys. Chem.* **1996**, *100*, 12489.
(15) Vailaya, A.; Horvath, C. *J. Phys. Chem.* **1997**, *101*, 5875.
(16) Park, S.-J.; Brendle, M. *J. Colloid Interface Sci.* **1997**, *188*, 336.
(17) Goss, K.-U. *J. Colloid Interface Sci.* **1997**, *190*, 241.
(18) Chaudhury, M. K.; Whitesides, G. M. *Langmuir* **1991**, *7*, 1013.
(19) Israelachvili, J. *J. Vac. Sci. Technol. A* **1992**, *10*, 2961.
(20) Israelachvili, J. N.; McGuiggan, P. M. *Science* **1988**, *241* (4867), 795.
(21) Biggs, S.; Mulvaney, P. *J. Chem. Phys.* **1994**, *100*, 8501.
(22) Milling, A.; Mulvaney, P.; Larson, I. *J. Colloid Interface Sci.* **1996**, *180*, 460.
(23) Veeramasuneni, S.; Hu, Y.; Yalamanchili, M. R.; Miller, J. D. *J. Colloid Interface Sci.* **1997**, *188*, 473.
(24) Ducker, W. A.; Senden, T. J.; Pashley, R. M. *Nature* **1991**, *353*, 239.
(25) Ducker, W. A.; Senden, T. J.; Pashley, R. M. *Langmuir* **1992**, *8*, 1831.
(26) Senden, T. J.; Ducker, W. A. *Langmuir* **1994**, *10*, 1003.
(27) Larson, D.; Drummond, C. J.; Chan, D. Y. C.; Grieser, F. *J. Phys. Chem.* **1995**, *99*, 2114.
(28) Binnig, G.; Quate, C. F.; Gerber, C. *Phys. Rev. Lett.* **1986**, *56*, 930.
(29) Frisbie, C. D.; Rozsnyai, L. F.; Noy, A.; Wrighton, M. S.; Lieber, C. M. *Science* **1994**, *265*, 2071.
(30) Noy, A.; Frisbie, C. D.; Rosznyai, L. F.; Wrighton, M. S.; Lieber, C. M. *J. Am. Chem. Soc.* **1995**, *117*, 7943.
(31) Vezenov, D. V.; Noy, A.; Rosznyai, L. F.; Lieber, C. M. *J. Am. Chem. Soc.* **1996**, *117*, 2006.

(32) Nakagawa, T.; Ogawa, K.; Kurumizawa, T.; Ozaki, S. *Jpn. J. Appl. Phys., Part 2* **1993**, *32*, L294.
(33) Nakagawa, T.; Ogawa, K.; Kurumizawa, T. *J. Vac. Sci. Technol. B* **1994**, *12*, 2215.
(34) Green, J.-B. D.; McDermott, M. T.; Porter, M. D.; Siperko, L. M. *J. Phys. Chem.* **1995**, *99*, 10960.
(35) Thomas, R. C.; Tangyunyong, P.; Houston, J. E.; Michalske, T. A.; Crooks, R. M. *J. Am. Chem. Soc.* **1995**, *98*, 4493.
(36) Green, J.-B.; McDermott, M. T.; Porter, M. D. *J. Phys. Chem.* **1996**, *100*, 13342.
(37) Sinniah, S. K.; Steel, A. B.; Miller, C. J.; Reutt-Robey, J. E. *J. Am. Chem. Soc.* **1996**, *118*, 8925.
(38) Schonherr, H.; Beulen, M. W. J.; Bugler, J.; Huskens, J.; van Veggel, F. C. J. M.; Reinhoudt, D. N.; Vansco, G. J. *J. Am. Chem. Soc.* **2000**, *122*, 4963.
(39) Skulason, H.; Frisbie, C. D. *J. Am. Chem. Soc.* **2000**, *122*, 9750.
(40) Ashby, P. D.; Chen, L.; Lieber, C. M. *J. Am. Chem. Soc.* **2000**, *122*, 9467.
(41) Schonherr, H.; Hruska, Z.; Vansco, G. J. *Macromolecules* **2000**, *33*, 4532.
(42) Skulason, H.; Frisbie, C. D. *Langmuir* **2000**, *16*, 6294.
(43) Schonherr, H.; Vansco, G. J. *J. Polym. Sci., Part B: Polym. Phys.* **1998**, *36*, 2483.
(44) Schonherr, H.; Hruska, Z.; Vansco, G. J. *Macromolecules* **1998**, *31*, 3679.
(45) Schonherr, H.; Vansco, G. J. *Macromolecules* **1997**, *30*, 6391.
(46) Feldmann, K.; Tervoort, T.; Smith, P.; Spencer, N. D. *Langmuir* **1998**, *14*, 372.

Experimental Section

Au- and Ag-Coated Substrates and Probe Tips. Substrates (Si (100) wafers, Silicon Sense, Nashua, NH; test grade, 500 μm thick) were coated in an electron-beam evaporator (base pressure 1×10^{-7} Torr) with a 50 Å adhesion layer of Cr followed by 1000 Å of Au at the rate of 1 Å/s. Commercial silicon nitride tip–cantilever assemblies (Digital Instruments, Santa Barbara, CA) were coated with Cr–Au as above or Cr–Ag deposited in a magnetron sputtering system, Vacuum Technologies, Inc. (base pressure 1×10^{-7} Torr, ~400 Å adhesion layer of Cr followed by approximately 2000 Å of Ag deposited at ~20 Å/s). Sputtering conditions were optimized to minimize the residual stresses separately in Ag and Cr layers and were as follows: 150 cm³-(STP) min^{-1} Ar gas flow, 2 mTorr pressure, pulsed DC plasma at 400 V. For consistency, the same evaporation conditions were used throughout this study.

Thiols used in the SAM preparation were purified by recrystallization or vacuum distillation. Thiolate monolayers were formed immediately after metal deposition by immersion of the freshly Au-coated substrates and Au- or Ag-coated probe tips in 2–3 mM EtOH solutions of functionalized long chain thiols for a least 2 h. Mixed monolayers of 16-mercaptoundecanoic acid and hexadecanethiol on AFM tips were formed by immersion in 1 mM (total concentration of thiol) EtOH solutions of varying composition for no longer than 2 h. Monolayer formation in all cases was verified by X-ray photoelectron spectroscopy (XPS) and contact angle measurements on flat Au- or Ag-coated Si substrates. The surface composition of mixed monolayers was determined from high-resolution XPS spectra of carbon and oxygen 1s region normalized by gold 4f peak.

The polymer for contact angle and AFM measurements was prepared by placing a drop of liquid prepolymer 10–12 mm in diameter onto a SAM substrate (SAM from 5–95% mixed solution of HS(CH$_2$)$_{15}$X, X = COOH, CH$_3$) and curing it in two steps: 3.5 h at 65 °C and 8 h at 130 °C. The prepolymer was prepared by melting, outgassing, and homogenizing a stoichiometric mixture of diglicidyl resorcinol ether and *m*-phenylenediamine at 65 °C. The final epoxy resin was completely cross-linked and had a glass transition temperature of 130 °C, Young's modulus of 3 GPa and yield stress of 150 MPa. The polymer remained in intimate contact with the substrate at all times until removed from it just prior to measurements. The surface roughness was 0.5 ± 0.1 nm over an area of 1 μm². For contact angle measurements, three freshly exposed polymer pieces were used and at least five measurements with each liquid were performed on each polymer substrate. Organic liquids were of the reagent grade or better. Water was deionized with a Barnstead NANOpure II filtration unit to 18 MΩ·cm resistivity.

Contact Angle Measurements. Contact angles were measured using a Rame–Hart Model 100 Goniometer at room temperature (22 ± 1 °C) and ambient humidity (60% relative humidity (RH)). At least 10 drops were evaluated for each liquid on homogeneous SAMs. Standard deviations for advancing and receding contact angles were 1–2°.

Chemical Force Microscopy. Au- and Ag-coated tips were inspected by a scanning electron microscope (SEM, Hitachi S800) to determine the tip radii and verify the intactness of the tip coating after experiments (Figure 3). Custom macro was written in image processing software (Optimas 6.1, Optimas Corp.) to fit a circle to three points specified on a contour of the tip apex profile taken at high magnification ($\times 60\,000$–$90\,000$). Observed radii were typically in the range of 50–150 nm, but occasionally much blunter tips ($R = 300$–400 nm) were observed. We estimate the uncertainty present in the evaluation of effective tip radii from SEM micrographs to be on the order of 20–30%, which is the main source of the error in the reported values for the work of adhesion and surface free energy.

Spring constants for 220 and 110 μm long cantilevers (V-shaped 20 μm wide NanoProbes from Digital Instruments, Inc., Santa Barbara, CA), determined using a nondestructive thermal resonance calibration method[47] were, on average, 0.11 ± 0.01 and 0.36 ± 0.02 N/m for Au-coated ones and 0.24 ± 0.02 and 0.46 ± 0.05 N/m for Ag-coated ones.

Adhesion measurements were made with a Nanoscope III Multi-Mode scanning force microscope (Digital Instruments) equipped with a fluid cell. Modified tips were rinsed in EtOH and dried with a stream of dry N$_2$ just prior to mounting them in the fluid cell. At least two modified tips were used for each type of measurement. The methodology of estimating the work of adhesion with chemically modified AFM tips has been outlined previously.[29,30] Briefly, the adhesive interaction between different functional groups was determined from force versus sample displacement curves. In these measurements, the deflection of the cantilever is recorded during the sample approach–withdrawal cycle. The observed cantilever deflection is converted into a force using the cantilever normal spring constant. The pull-off force in the sample retracting trace corresponds to the adhesion between functional groups on the tip and sample surface. All force versus distance curves were captured using Nanoscope III software and later analyzed using a set of custom procedures written for IGOR Pro 3.1 data analysis software (WaveMetrics Inc., Lake Oswego, OR). The adhesion force was independent (with random scatter around the average) of the maximum contact force applied in the approach–withdrawal cycle (up to 3 times the adhesion force value). Average adhesion force values were determined from histograms of the adhesion values obtained from at least 200 individual force measurements.

Superlayer Test Measurements of Interface Fracture Energy.[48] Microlines of the polymer were capillary-molded on the top of the SAM, and the Au/Si substrate between the lines was slightly etched. Separation between SAM and epoxy lines was induced by depositing a highly stressed Ni overlayer on the top of the lines. The interface crack always arrested before it reaches the end of the line. The length of the remnant, an attached ligament, yields an accurate measurement of interfacial fracture energy.

Results and Discussion

Adhesion Forces in Media of Different Polarity. We[30,31,49] and others[37,50] have found that adhesion forces between the same functional group pairs can differ in media of different polarity (alcohols, water, and hydrocarbons). Table 1 exemplifies the dramatic effect of medium composition on adhesion between two methyl surfaces. The force of adhesion increases as one proceeds from hydrocarbons to alcohols, to even more polar solvents such as nitriles, oxides, amides, diols, and water. The same tip–substrate pair was used in this experimental series. The geometrical parameters were thus preserved from solvent to solvent, and the observed changes in adhesion are due only to a differing composition of the medium. The trend of higher forces between CH$_3$ groups in more polar solvents is in accordance with the chemical intuition that the creation of a nonpolar/polar interface is energetically unfavorable. Table 1 shows the effect of changing the solvent polarity on the contact (adhesive) interactions between self-assembled monolayers terminating in CH$_3$ groups. An inspection of adhesion force variation in Table 1 with the properties of the solvent relating to its polarity or cohesive energy density does not immediately reveal a clear relationship. To understand the details of the solvent effect on adhesion and to quantify its influence, we have conducted a systematic study using a series of solvents with a varying degree of hydrogen-bonding ability (methanol–water mixtures). The medium effect is manifested by the changes in the effective Hamaker constant, *A*, which is estimated from the

(47) Hutter, J. L.; Bechhoefer, J. *Rev. Sci. Instrum.* **1993**, *64*, 1868.
(48) Zhuk, A. V.; Evans, A. G.; Hutchinson, J. W.; Whitesides, G. M. *J. Mater. Res.* **1998**, *13*, 3555.
(49) Noy, A.; Vezenov, D. V.; Lieber, C. M. *Annu. Rev. Mater. Sci.* **1997**, *27*, 381.
(50) Clear, S.; Nealey, P. F. *J. Colloid Interface Sci.* **1999**, *213*, 238.

Table 1. Scaled Experimental Work of Adhesion (Water = 100) between CH_3-Terminated SAMs in a Series of Solvents with Different Polarity and Hydrogen Bonding

medium	adhesion	dipole moment (D)	dielectric constant	surface tension (mJ/m^2)	vdW surface tension (mJ/m^2)	Hildebrand parameter ($(cal/cm^3)^{1/2}$)
decane	0.33	0	1.99	23.9	23.9	8.0
benzene	0.38	0	2.28	28.9	27.1	9.2
propanol	1.54	1.68	20.1	23.3	21.1	11.9
butanol	1.64	1.66	17.8	25.0	24.6	11.4
hexanol	2.01	1.61[a]	13.3	25.8	25.8[a]	10.7
ethanol	2.07	1.69	24.3	22.8	20.1	12.7
methanol	4.35	1.70	33.6	22.6	18.5	14.5
DMF	5.14	3.82	36.7	36.7	36.7[b]	12.1
acetonitrile	10.3	3.92	38.0	29.3	29.3[b]	12.0
DMSO	14.5	3.96	45.0	44	36	12.0
ethylene glycol	25.8	2.28	37.7	48.2	29	14.6
water	100	1.85	80.4	72.4	21.8	23.4

[a] Extrapolated based on values in homologous series. [b] Dispersion component of surface tension set equal to total surface tension, since there are no acceptor sites in the molecule.
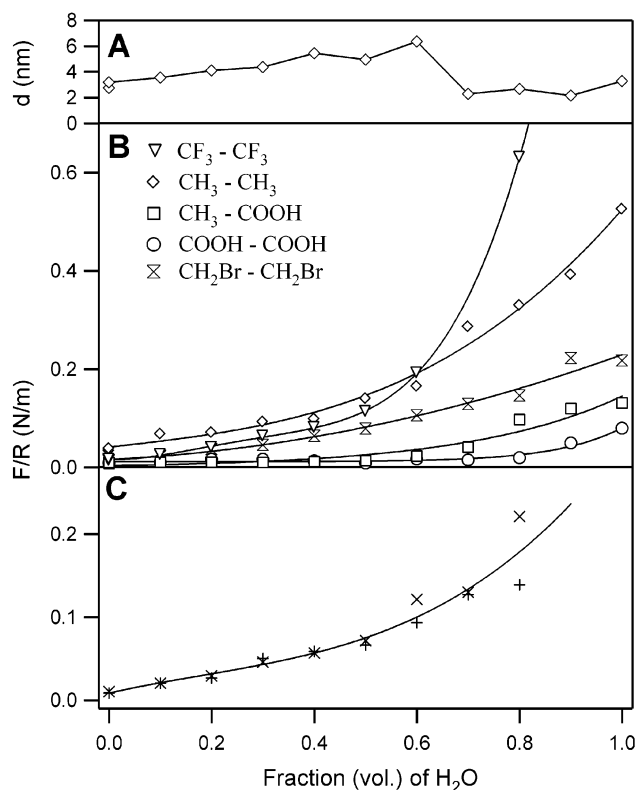

Figure 1. Results of CFM experiments in methanol−water solvents. (A) Jump to contact distances, *d*, for tip and substrates functionalized with methyl-terminated SAMs (standard deviation of the measurement of *d* in a given solvent was, on average, 1.8 nm). (B) Adhesion forces normalized by the tip radii for tip−samples bearing CH_3, CF_3, Br, and COOH groups (standard deviations are summarized in Figure 6) and (C) epoxy polymer and methyl SAM as a function of solvent composition (× and + correspond to two different tips).

distance, *d*, at which the AFM tips of radius *R* jumps into intimate contact with the sample surface (*k* is the cantilever stiffness):

$$A = \frac{kd^3}{3R} \qquad (1)$$

As seen from the data in Figure 1A, on going from methanol to water, there are only small fluctuations around an average value of 4 nm, corresponding to an effective Hamaker constant of approximately 40×10^{-20} J·m. Similar behavior (<20%

change of $d \approx 3-4$ nm) was observed for CH_3/COOH and COOH/COOH pairs, although for the CF_3/CF_3 pair the snap-in distance gradually increased from 0.3 to 4 nm. The value of the Hamaker constant is typical of that found for the Au−water−Au system. This behavior is expected, since dielectric properties of a SAM and organic solvents are very similar.[1,2] Thus, interaction at large distances (>3 nm) is dominated by two metal layers, while at contact it decreases to less than 10% of the total work of adhesion. Experiments with SAMs of different chain lengths confirm this interpretation. Adhesion in methanol between samples that have been modified with HS-$(CH_2)_nCH_3$ ($n = 11, 15, 21, 25$) and tips modified with a HS-$(CH_2)_{15}CH_3$ SAM shows only small differences as a function of chain length: 0.53 ± 0.16 ($n = 11$), 0.57 ± 0.16 ($n = 15$), 0.47 ± 0.13 ($n = 21$), and 0.45 ± 0.12 nN ($n = 25$). The jump-to-contact distance reproduced the change in SAM chain length (change of -0.73 ± 0.09 Å per additional CH_2 group) and is a result of the shift in the plane of hard contact with respect to two metal layers: 3.15 ± 0.50 ($n = 11$), 3.00 ± 0.37 ($n = 15$), 2.39 ± 0.36 ($n = 21$), and 2.21 ± 0.29 nm ($n = 25$).

By contrast, variation in the solvent polarity in methanol−water solutions resulted in a clear trend in measured adhesion forces between tips and substrates coated with self-assembled monolayers terminated in $-CH_3-CF_3-CH_2Br$, and −COOH groups (Figure 1B). For each functional group pair, the experiments were carried out with the same arrangement of tip and sample by exchanging the solvent in the microscope fluid cell. The results clearly demonstrate that the covered medium can have a pronounced effect on adhesion between two SAM surfaces. Since the nonpolar monolayers ($-CH_3$ and $-CF_3$) are not capable of participating in polar interactions (primarily hydrogen bonding) with the solvent (water or methanol), the order of magnitude increase in adhesion forces at higher water content results from the *intrasolvent* polar interactions. This apparently counterintuitive conclusion while dealing with surfaces is supported by detailed consideration of energy balance in the system as developed below: in order to create a SAM−solvent interface some solvent−solvent bonds need to be broken. A similar type of behavior in the mixed alcohol−water solvent series was observed with more complex organic surfaces, e.g. when epoxy polymer was used as a substrate (Figure 1C). Adhesion between the methyl terminated tip and epoxy increased severalfold as the solvent mixture became more water rich. We[49] and others[50] have previously demonstrated that the

adhesion values in pure solvents can be quantitatively predicted on the basis of the surface tension component theory.[4,5,7,8] As shown below, the systematic change in the degree of hydrogen bonding (in the free energy sense) in the SAM−mixed solvent−SAM or mixed SAM−polymer−water systems can change the measured adhesion force by an order of magnitude. The change can be accounted for in terms of surface tension component theory.

Intermolecular Force Components Theory: Determination of Surface Free Energies with Contact Angles of Alcohol−Water Mixtures on Apolar Solids. The surface energetics in these systems can also be derived from contact angle measurements for low energy surfaces ($-CH_3$ and $-CF_3$). In the case of apolar solids, a simple interpretation based on a surface tension component approach by Fowkes, van Oss, Chaudhury, and Good (FOCG)[4,5,7,8] can be given to observed values of contact angles of alcohol−water mixtures. The total surface tension of a polar system is separated into van der Waals, γ^{vW}, and Lewis acid, γ^+, and base, γ^-, components:

$$\gamma_{total} = \gamma^{vW} + \gamma^{AB} \qquad (2)$$

where $\gamma^{AB} = 2\sqrt{\gamma^+ \gamma^-}$. The solid−liquid interfacial tension, according to the FOCG method, is then given by

$$\gamma_{SL} = (\sqrt{\gamma_{LV}^{*vW}} - \sqrt{\gamma_{SV}^{vW}})^2 + 2(\sqrt{\gamma_{LV}^{*+}\gamma_{LV}^{*-}} + \sqrt{\gamma_{SV}^+\gamma_{SV}^-} - \sqrt{\gamma_{LV}^{*+}\gamma_{SV}^-} - \sqrt{\gamma_{SV}^+\gamma_{LV}^{*-}}) \quad (3)$$

where a different composition at the solid−liquid interface for a mixed solvent is taken into account by employing appropriate liquid surface tension $\gamma_{LV}^* \neq \gamma_{LV}$ (reflecting surface composition different from the bulk) for use with the geometric mean combining relationship. With completely apolar surfaces, the last two terms in eq 3 are zero (i.e. $\gamma^{AB} = \gamma^+ = \gamma^- = 0$) and for alcohol−water systems, we arrive at the following relationship governing contact angles on apolar substrates:

$$\gamma_{LV} \cos\theta = \gamma_{SV} - \gamma_{SL} = 2\sqrt{\gamma_{SV}\gamma_{LV}^{*vW}} - \gamma_{LV}^* \qquad (4)$$

When Young's equation is combined with the Gibbs adsorption isotherm,[51] a linear correlation between $\gamma_{LV} \cos\theta$ and γ_{LV} is observed (Figure 2A):

$$\frac{d(\gamma_{LV} \cos\theta)}{d\gamma_{LV}} = \frac{\Gamma_{SV} - \Gamma_{SL}}{\Gamma_{LV}} \qquad (5)$$

where Γ_{ij} is the adsorption of a low-energy component (alcohol) at the ij interface.

Assuming that adsorption from the vapor phase on the solid is negligible compared to the other two interfaces, the negative of the slope of the curves in Figure 2A gives the ratio of adsorption of alcohol at the solid−liquid interface to its adsorption at the liquid−vapor interface. The fact that such ratios are constant over a wide concentration range was also noticed for solutions of surfactants[51] and proteins.[52] As seen from the data in Table 2 the composition of a liquid phase contacting a
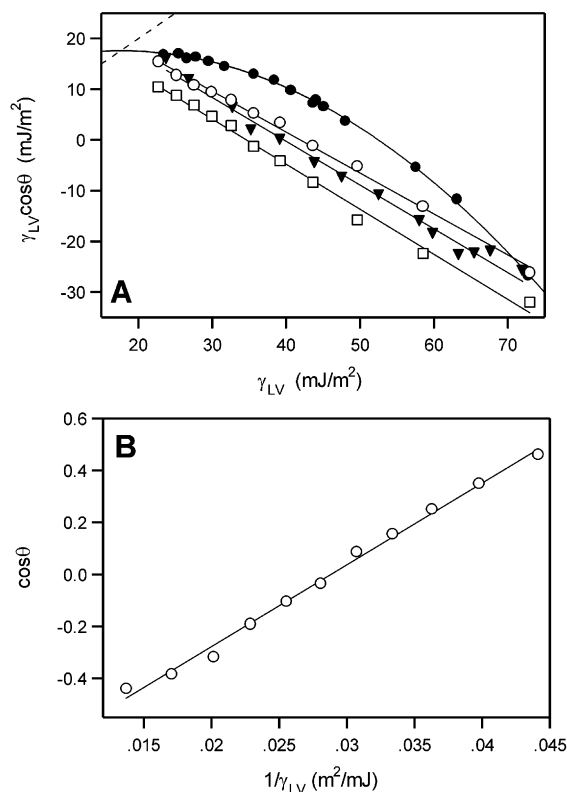
(51) Lucassen-Reynders, E. H. *J. Phys. Chem.* **1963**, *67*, 969.
(52) Van der Vegt, W.; Van der Mei, H. C.; Busscher, H. J. *J. Colloid Interface Sci.* **1993**, *156*, 129.

Figure 2. (A) Plot of $\gamma_{LV} \cos\theta$ versus γ_{LV} for alcohol−water mixtures on hydrophobic substrates: methanol−water on $-CH_3$ (□) and CF_3 (○) SAMs. Literature data for pure solvents[56] (●) and propanol−water (▼) on Teflon[54] are also shown for comparison. Dashed line corresponds to a condition of complete wetting $\gamma_{LV} \cos\theta = \gamma_{LV}$. (B) Plot of $\cos\theta$ versus $1/\gamma_{LV}$ for mixed methanol−water solvents on a CF_3-terminated SAM surface.

low-energy surface or vapor is practically the same ($\Gamma_{SL} \approx \Gamma_{LV}$) and, therefore, γ_{LV}^* does not deviate significantly from γ_{LV}.

Despite the varying composition at the interface, γ_{LV}^{*vW} can be taken constant at 20 ± 1.5 mJ/m^2, because γ^{vW} values for water and alcohols are very close (21.8, 18.5, and 20.1 mJ/m^2 for water, MeOH, and EtOH, respectively). Combining $\gamma_{LV}^{*vW} \approx$ constant with the condition $\gamma_{LV}^* \approx \gamma_{LV}$, as discussed above, we obtain a linear relationship between $\cos\theta$ and $1/\gamma_{LV}$ (originally noticed in experiments for solutions of surfactants[51]):

$$\cos\theta = -1 + 2\sqrt{\gamma_{SV}\gamma_{LV}^{*vW}}\frac{1}{\gamma_{LV}} \approx -1 + \frac{constant}{\gamma_{LV}} \qquad (6)$$

The linear correlation between contact angles and $1/\gamma_{LV}$ is, indeed, observed over the whole range of alcohol concentrations for CH_3 and CF_3 SAMs (Figure 2B). Literature values for paraffin[53] and Teflon[54] follow the same law and the intercepts are close to -1 (-0.94 and -0.97 for paraffin and Teflon, for example). The values of γ_{SV} estimated from the slopes are shown in Table 2. This analysis can be extended to cases when Lewis acid−base interactions between solid and liquid components are present and/or when liquids with substantially different γ^{vW} are used. The combining relationship (eq 3) should

(53) Dann, J. R. *J. Colloid Interface Sci.* **1970**, *32*, 302.
(54) Tronel-Peyroz, E.; Lhassani, A. *J. Colloid Interface Sci.* **1995**, *171*, 522.
(55) Bain, C. D.; Troughton, E. B.; Tao, Y.-T.; Evall, J.; Whitesides, G. M.; Nuzzo, R. G. *J. Am. Chem. Soc.* **1989**, *111*, 321.
(56) Li, D.; Neumann, A. W. *J. Colloid Interface Sci.* **1992**, *148*, 190.

Table 2. Surface Free Energy of Nonpolar Solids Determined From Contact Angles with a Range of Mixed Alcohol−Water Solvents (Me = Methyl, Et = Ethyl, Pr = Propyl, Bu = Butyl)

surface	liquid	Γ_{SL}/Γ_{LV}	γ_{SV}(expt)	γ_{SV}(lit.)	ref
paraffin	BuOH−H_2O and EtOH−H_2O	0.86	26	25	53, 54
Teflon	PrOH−H_2O and EtOH−H_2O	0.95	21	22	53, 54
Au−$S(CH_2)_{16}CH_3$	MeOH−H_2O	0.81	15	19	55
Au−$S(CH_2)_{16}CF_3$	MeOH−H_2O	0.89	13	12	55
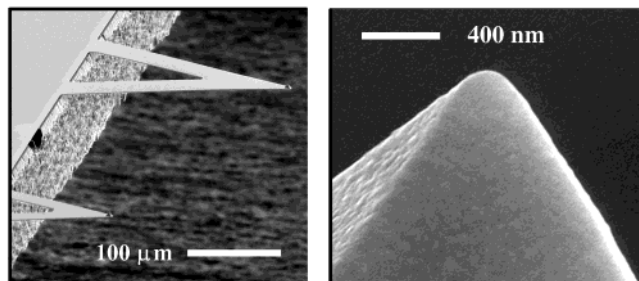
Figure 3. Scanning electron microscopy images of Ag-coated cantilever−tip assemblies, showing uniform coverage, absence of residual stress in the metal coating, and approximately spherical shape of the tip apex.

then be modified by taking into account the chemical heterogeneity of the surfaces in contact, whose composition can be calculated from an experimental Γ_{SL}/Γ_{LV} ratio.

Thus, the change in the solvent hydrogen bonding ability (given by $\gamma_{total} - \gamma^{vW}$) through a continuous change in composition can bring about significant changes in solid−liquid interfacial free energy for low-energy organic surfaces (from 2 to 50 mJ/m^2 as calculated from the contact angle data presented here). The experimental contact angles in this case are amenable to interpretation in terms of the FOCG approach. In adhesion measurements with sharp tips, the main contribution to tip−surface interaction forces comes from the layer of solvent in intimate contact with surface groups, and thus the values of solid−liquid interfacial free energy derived from the above contact angle measurements should be adequate thermodynamic quantities to assist in the interpretation of adhesion data.

Interpretation of Adhesion Force Measurements with Continuum Contact Mechanics Models. The direct relationship between γ_{SL} from contact angles and adhesion from force measurements is intuitively expected, and the contact mechanics approach can be used to analyze the force microscopy data. Figure 3 shows SEM images of Ag-coated tips. In the first approximation, the tip apex which comes in contact with the sample during force measurements can be treated as spherical. The measured adhesive forces in solution have been previously found[29−31] to agree with predictions of the Johnson−Kendall−Roberts (JKR) theory[57] and thus show that the adhesion data can be directly linked to the surface free energy and the energetics of the different intermolecular interactions. There are indications from self-consistent calculations[58] that deformations at this scale are unimportant (Derjaguin−Muller−Toporov (DMT) regime[59]).

The pull-off force, F_{ad}, required to separate a tip of radius R from a planar surface is directly proportional to the thermodynamic work of adhesion, W_{SLT}, for separating the sample and tip:

$$F_{ad} = n\pi R W_{SLT} \qquad 3/2 \text{ (JKR)} < n < 2 \text{ (DMT)} \qquad (7)$$

where

$$W_{SLT} = \gamma_{SL} + \gamma_{TL} - \gamma_{ST} \qquad (8)$$

and γ_{SL} and γ_{TL} are the surface free energies of the sample (S) and tip (T), respectively, in contact with the liquid (L) and γ_{ST} is the interfacial free energy of the two contacting solid surfaces. In the case of symmetrical interactions, $\gamma_{ST} = 0$ and $\gamma_{SL} = \gamma_{TL}$, and eq 7 simplifies to $W_{SLT} = 2\gamma_{SL}$. It is, therefore, the solid−liquid surface free energy that should determine the adhesive force between tip and sample pairs modified with the same molecular groups. Our experimental data do not allow one to claim an exact value of the numerical coefficient in eq 7 (3/2 vs 2) due to the experimental uncertainty (standard deviation of adhesion force distribution plus errors in the determination of k and R). The validity of the combined use of the contact mechanics and Young's equations has been previously verified with adhesion force measurements between macroscopic elastomeric lenses in methanol−water mixtures.[18] Our data support this conclusion for nanometer sized contacts as well.

Combining results on adhesion force measurements with the contact angle data on low-energy CH_3 monolayers, we observed that there is a direct, almost linear, correlation between adhesion forces and corresponding surface free energy values determined with contact angles (Figure 4A). This correlation was always present independent of the type of the metal coating (Au or Ag). Occasionally, for CH_3−CH_3 interactions the force versus surface free energy curves had a nonlinear shape (Figure 4B). Although the force continued to increase with the higher water content, there was a change in the slope of the curves above ∼50 nN. This inflection could be attributed to a breakdown in the approximation of small deformations as assumed by contact mechanics models. In addition, as the forces increase, new areas of the tip are involved in contact with and deformation by the substrate, thus altering the effective tip radius, which may involve several Ag or Au grains. If the tip apex is not axially symmetric, the pull-off force depends on the free energy in a more complex way than linear.[60] The calculated average contact pressure developing at these forces is approximately 0.15−0.75 GPa (for $R \sim 200$ nm, $K \sim 60$ Gpa, and $F_{ad} \sim 1-100$ nN), which is below the level at which displacement of thiol molecules may occur (2.3 GPa).[61] A considerable deformation of the monolayer or Au (Ag) substrate may, however, also be the cause of the nonlinearity observed at higher adhesion forces.

(57) Johnson, K. L.; Kendall, K.; Roberts, A. D. *Proc. R. Soc. London A* **1971**, *324*, 301.
(58) Muller, V. M.; Yushchenko, V. S.; Derjaguin, B. V. *J. Colloid Interface Sci.* **1980**, *77*, 91.
(59) Derjaguin, B. V.; Muller, V. M.; Toporov, Y. P. *J. Colloid Interface Sci.* **1975**, *53*, 314.
(60) Chaudhury, M. K.; Weaver, T.; Hui, C. Y.; Kramer, E. J. *J. Appl. Phys.* **1996**, *80*, 30.
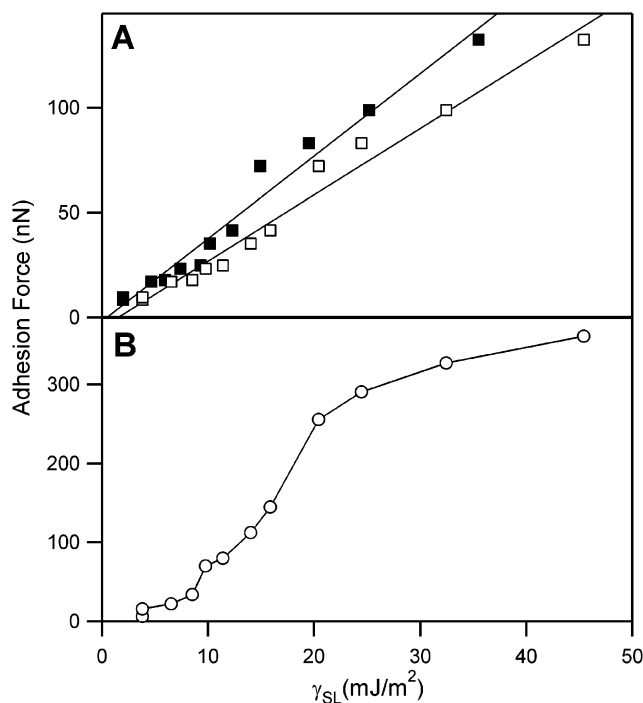(61) Lio, A.; Morant, C.; Ogletree, D. F.; Salmeron, M. *J. Phys. Chem. B* **1997**, *101*, 4767.

Figure 4. (A) Adhesion between $-CH_3$-terminated tips and samples versus solid$-$liquid surface free energy determined from advancing (open symbols) and receding (closed symbols) contact angles, using 19.3 mJ/m^2 for γ_{SV} for CH$_3$ SAM. (B) Nonlinear relationship occasionally observed for adhesion force between $-CH_3$-terminated tips and samples and solid$-$liquid surface free energy determined from contact angles.

It is possible to use these data in the low-force regime to check the validity of the $\gamma_{ST} = 0$ assumption in the case of identical nonpolar functional groups on the tip and sample, e.g. CH$_3-$CH$_3$ interactions. It is apparent that the linear fit in Figure 4 does not go through the origin, and thus the work of adhesion of $\sim$2 mJ/m^2 at $F_{adh} = 0$ nN will correspond to the value of the interfacial tension between the identical surface groups. When adhesion data are taken with the same tip$-$sample pair, γ_{SL} and, hence, F_{ad} are directly proportional to $\gamma_{LV} \cos \theta$ (Figure 5):

$$F_{ad} = 2n\pi R\gamma_{SL} = 2n\pi R(\gamma_{SV} - \gamma_{LV} \cos \theta) \qquad (9)$$

Plots of $\gamma_{LV} \cos \theta$ versus F_{ad} extrapolated to zero adhesion force yield γ_{SV} (less $\gamma_{ST}/2$). We have used this approach for CH$_3$-terminated SAMs to obtain a value of $\gamma_{SV} = 17 \pm 1$ mJ/m^2 for advancing and 18 ± 1 mJ/m^2 for receding contact angles (the average represents data from six different experiments) in close agreement with the value of 19.3 mJ/m^2 reported by Bain et al.[55] Therefore, the choice of $\gamma_{ST} \approx 0$ appears to be justified for apolar SAMs ($\gamma_{ST} \leq 2$ mJ/m^2). This small value of γ_{ST}, together with the linearity of the plots in Figure 5, suggest that no solvent molecules are present in the contact zone between the tip and the sample.

Role of Hydrogen Bonding Interactions. We conclude that the contact mechanics approach can estimate the free energy of the sample$-$solvent interface. The experimental data on forces between SAMs in methanol$-$water (Figure 1) suggest that the adhesion between organic surfaces will be lower in associating solvents, if such surfaces are capable of participating in the hydrogen bonding with the solvent. Moreover, since this series of solvents has a practically constant contribution to dispersion interactions, the solvation of surface groups through polar
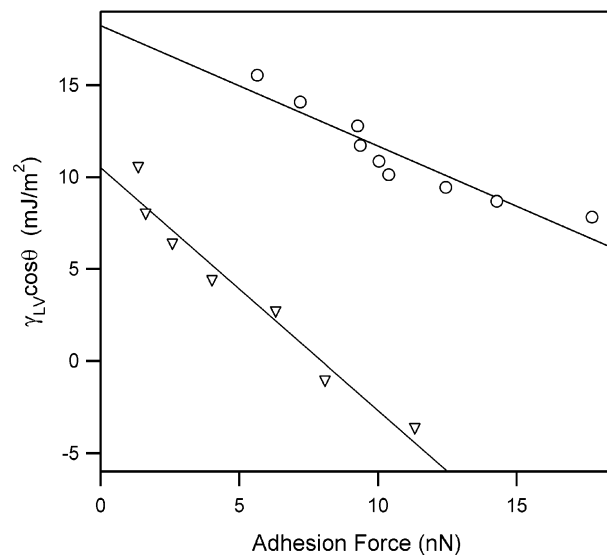
Figure 5. Plots of $\gamma_{LV} \cos \theta_{adv}$ versus adhesion force for the determination of γ_{SV} values for SAMs terminating in CH$_3$ (circles) and CF$_3$ (triangles) groups. Values of $\gamma_{SV} = 18.5$ (for CH$_3$) sand $\gamma_{SV} = 10.8$ mJ/m^2 (for CF$_3$) are determined by extrapolation to zero adhesion force.

interactions becomes the most crucial factor in determining the magnitude of adhesion forces. For nonpolar surfaces, intrasolvent interactions appear to have a pronounced effect and are responsible for an order of magnitude change in adhesion: free energy changes due to breaking solvent$-$solvent contacts in order to create a SAM$-$solvent interface are not fully compensated by interactions at the SAM$-$solvent interface. If at least one of the interfaces is able to maintain hydrogen bonding with the solvent (e.g. CH$_3-$COOH and COOH$-$COOH pairs in Figure 1), the effect of strong intrasolvent interactions is offset by hydrogen bonding at the interface. Water, with its exceptional hydrogen bonding properties (both as acceptor and donor), used as a solvent in CFM measurements will, therefore, discriminate best between various organic groups, a fact also pointed out by others.[37]

The role of the solvent in determining the values of adhesion force can be rationalized in a semiquantitative fashion by using the FOCG model for surface tensions. As mentioned in the previous section, the last three terms in eq 3 are zero for CH$_3$-terminated SAMs (i.e. $\gamma^{AB} = \gamma^+ = \gamma^- = 0$), while the van der Waals component determined from contact angle measurements with liquid hydrocarbons (19.3 mJ/m^2) is essentially the same as the corresponding values obtained with alcohols and with water (21.8, 18.5, and 20.1 mJ/m^2 for water, MeOH, and EtOH, respectively).[7] Thus, the first term in eq 3 is also negligible, and the value of the adhesion force between two methyl surfaces in alcohol (water) is essentially a measure of the strength of the hydrogen bonding interaction (in a free energy sense) in liquid alcohol (water):

$$W_{CH_3-ROH-CH_3} = 2\gamma^{AB}_{ROH} \qquad (R = C_2H_5, CH_3, \text{ or } H) \quad (10)$$

Ethanol and methanol have essentially indistinguishable values of surface tension (22.8 and 22.6 mJ/m^2, respectively) but different hydrogen bonding components ($\gamma^{AB} = 2.7$ and 4.1 mJ/m^2, respectively), both of which are much smaller than the corresponding value for water ($\gamma^{AB} = 51$ mJ/m^2). When the same tip and sample are used in the adhesion experiment, forces

between CH$_3$ groups in MeOH were consistently 1.5−2 times greater than those in EtOH, in agreement with the ratio of 1.6 between corresponding γ^{AB} values, and adhesion increased by more than an order of magnitude (from 4−8 to 100−300 nN) when water was introduced as one of the components of the intervening solvent (Figure 1).

The FOCG model also predicts that adhesion measurements made in a nonpolar or monopolar solvent (e.g. such that $\gamma^+ = 0$) with surface tensions close to that of the CH$_3$-terminated SAMs should be very small. Indeed, in ethyl acetate ($\gamma = 23.9$ mJ/m^2) adhesion forces were nearly indistinguishable from the background ($\sim$0.1 nN). Ethylene glycol (EG) and dimethyl sulfoxide (DMSO) present another example of two solvents with a similar surface tension (48 and 44 mJ/m^2), but quite different adhesion forces between apolar surfaces. These solvents have significant acid−base components (19 and 8 mJ/m^2, respectively) and dispersion contributions that differ from that of the CH$_3$-terminated SAM (29 and 36 mJ/m^2, respectively).[7] Adhesive forces between methyl surfaces in EG are predicted (eqs 6 and 9) to be greater than those in DMSO by a factor of 1.8, while our experiments yielded a factor of 1.8−2.0 difference. These data independently confirm the validity of the intermolecular force components approach for treating the adhesive interactions in solvents. A similarly good correlation between the work of adhesion for CH$_3$-terminated SAMs obtained from CFM experiments and the FOCG model was reported for the solvent series involving hexadecane, ethanol, 1,2- and 1,3-propanediol, and water.[50]

Although the macroscopic surface free energy appears to correlate well with the nanoscopic adhesion force, the number of species involved in the interaction is small in a thermodynamic sense. Thus, large fluctuations are expected in values of adhesion force determined from the individual measurements due to variations in the number of ruptured bonds (n) and/or strength of the individual bond (F_s) (because of the differences in molecular alignment, rate of separation, etc.).[62−65] The width of distribution (σ_F) of adhesion force tends to increase for higher mean values of force (μ_F). Figure 6 shows the resulting correlation between widths of distribution of adhesion force and the average values of adhesion force for the data shown in Figure 1.

The number of ruptured single bonds can unambiguously be determined when discreteness (periodicity) of the adhesion force distribution is detected[39] or ensured by spacing (re)active components apart.[66] For functional group assemblies, a statistical analysis of the discrete bond rupture process was suggested[62] to yield a single bond strength $F_s = \sigma_F^2/\mu_F$ on the basis of the properties of the Poisson distribution ($\sigma_n^2 = \mu_n$ for the number of bonds). While an agreement was found between single bond values obtained in that way and single bond values determined using estimates of the contact *area* at pull-off,[67] the above analysis of the pull-off forces in polar solvents requires these
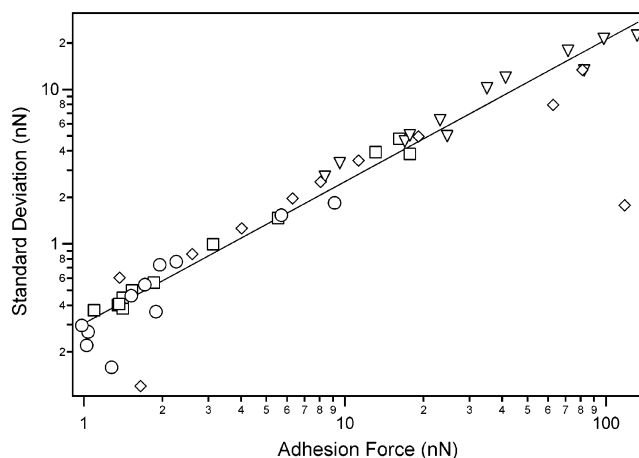

Figure 6. Variation of the widths of the distributions of adhesion force with the mean value of this force for tip and samples presented in Figure 1B.

single bond values to be viewed as weighted average forces that include several individual types of single bonds: those between tip and sample molecular groups, between solvent molecules, and between solvent molecules and tip or sample groups. This is especially true of the CFM measurements in solvents with hydrogen bonding (such as alcohols). The refined statistical treatment will need to take into account additional bonds breaking in the interaction *volume* around the tip−sample juncture. For the data in Figure 6, the phenomenological exponent k in the relation $\sigma_F \sim \mu_F^k$ is 0.9, rather than 0.5 as previously found.[62−65]

The empirical finding from the data presented in Figure 6 is that larger forces (energies) are also characterized by wider distributions for all terminal functional groups. The apparent low sensitivity to the exact nature of the terminal functional group is likely due to the dominant role of the hydrogen bonding of type OH···O for the systems studied, whether the distribution in pull-off force is due to variations in the number or the strength of the single bonds broken.

Thermodynamic Work of Adhesion in the Epoxy−Water−SAM System. The approaches developed above can be applied to a much more complex system to gain some understanding of the trends in adhesion force between polar organic substrates in a polar medium. We analyzed the behavior of synthetic epoxy polymer in contact with SAMs of varying hydrogen bonding ability in the presence of a hydrogen bonding solvent, water.

Surface Free Energy of the Polymer Determined with Probe Liquids. The polymer used in this study is highly cross-linked and was synthesized according to the reaction
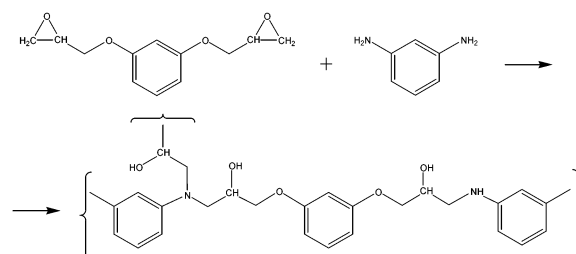
Since this epoxy resin has a large number of polar hydroxyl and amino groups, its interfacial tension with a COOH/CH$_3$

(62) Han, T.; Williams, J. M.; Beebe, T. P., Jr. *Anal. Chim. Acta* **1995**, *307*, 365.
(63) Wenzler, L. A.; Moyes, G. L.; Raikar, G. N.; Hansen, R. L.; Harris, J. M.; Beebe, T. P., Jr.; Wood, L. L.; Saavedra, S. S. *Langmuir* **1997**, *13*, 3761.
(64) Wenzler, L. A.; Moyes, G. L.; Olson, L. G.; Harris, J. M.; Beebe, T. P., Jr. *Anal. Chem.* **1997**, *69*, 2855.
(65) Williams, J. M.; Han, T.; Beebe, T. P., Jr. *Langmuir* **1996**, *12*, 1291.
(66) Grandbois, M.; Beyer, M.; Rief, M.; Clausen-Schaumann, H.; Gaub, H. E. *Science* **1999**, *283*, 1727.
(67) Van der Vegte, E. W.; Hadziioannou, G. *Langmuir* **1997**, *13*, 4357.

Table 3. Surface Tension Components of Probe Liquids and Their Contact Angles (CA) on Epoxy Polymer

liquid	γ_L, mJ/m²	γ^{vW}, mJ/m²	γ^+, mJ/m²	γ^-, mJ/m²	CA, deg
water (W)	72.8	21.8	34.2	19	74.9 ± 3.0
glycerol (Gly)	64	34	5.3	42.5	65.2 ± 4.2
ethylene glycol (EG)	48	29	2.6	34.8	49.1 ± 1.7
dimethyl sulfoxide (DMSO)	44	36	0.7	23.8	29.5 ± 1.5
diiodomethane (DM)	50.8	50.8	−	−	41.6 ± 3.5

Table 4. Surface Tension Components of Epoxy Polymer Determined from the Contact Angles of Probe Liquids[a]

Liquids	γ^{vW}, mJ/m²	γ^+, mJ/m²	γ^-, mJ/m²	γ^{AB}, mJ/m²	γ_E, mJ/m²
DM-W-Gly	38.8	0.27	6.2	2.7	41.5
DM-W-EG	38.8	0.11	6.9	1.7	40.5
DM-W-DMSO	38.8	0.10	6.9	1.7	40.5
DM-DMSO-Gly	38.8	0.03	11.7	1.3	40.2
DM-DMSO-EG	38.8	0.10	7.1	1.7	40.5
DMSO-W-Gly	33.2	0.82	6.6	4.6	37.8
DMSO-W-EG	38.6	0.12	6.9	1.8	40.4
mean (±1 σ)	38.0 ± 2.1	0.22 ± 0.27	7.5 ± 1.9	2.2 ± 1.1	40.2 ± 1.1

[a] Liquids are defined in Table 3.

mixed SAM as well as water solvent is expected to be influenced to a large extent by acid−base interactions. The work of adhesion between a solid surface, S, and liquid, L, in the Young−Dupre equation is given by

$$\gamma_L(1 + \cos\theta) = W_{SL} = W_{SL}^{vW} + W_{SL}^{AB} =$$
$$2[\sqrt{\gamma_S^{vW}\gamma_L^{vW}} + \sqrt{\gamma_S^+\gamma_L^-} + \sqrt{\gamma_L^+\gamma_S^-}] \quad (11)$$

One nonpolar liquid can be used to determine γ^{vW}, and two more (polar) liquids with known γ^+ and γ^- components are required to fully characterize the solid surface free energy of the polymer by means of eq 11. The surface tension components for five liquids and their contact angles with epoxy polymer are presented in Table 3. The surface free energy components of the polymer derived from these measurements are summarized in Table 4. The numbers are consistent with the chemical structure of the epoxy resin, which can be described as strongly basic (due to a large number of electron donors, such as O and N atoms and benzene rings) and weakly acidic (due to the presence of OH groups).

Surface Free Energy of the Polymer Determined with Model SAMs. As seen from the data in Table 2, $\gamma_E = 40.2 \pm 1.1$ mJ/m² is the best estimate of the surface tension of epoxy polymer, based on measurements of the contact angle using polar liquids. This value can be confirmed independently by using the contact angle of epoxy polymerized on a nonpolar CH₃-terminated SAM. The dispersion component of CH₃-terminated SAMs determined from contact angle measurements with liquid hydrocarbons is 19.3 mJ/m².[55] The application of eq 11 to this case leads to ratio $(\gamma_E^{vW})^{0.5}/\gamma_E = 0.140$ and $\gamma_E = 44.0$ mJ/m² for γ_E^{vW} value of 38.0 mJ/m² from Table 4.

Moreover, we are able to infer the surface free energy of the polymer from the set of contact angle data with mixed SAMs of known surface composition. Mixed CH₃−COOH SAM surfaces were prepared, and a surface fraction of COOH groups was determined from XPS spectra. A drop of liquid prepolymer was placed on the SAM surface and polymerized. Contact angles of the polymer on the SAM samples thus obtained were then measured.

Cosines of equilibrium contact angles of liquids, cos θ, on heterogeneous surfaces with well-defined surface regions (patches)
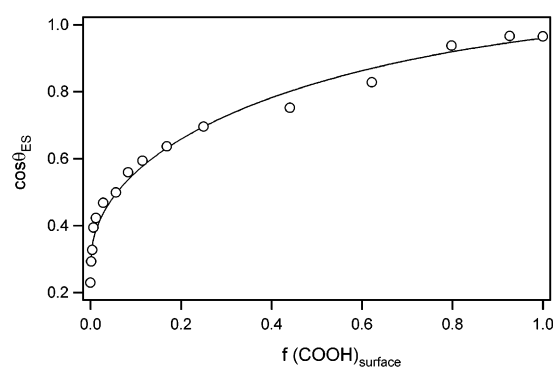

Figure 7. Nonlinear relationship observed between cosine of contact angle, cos θ_{ES}, of epoxy polymer on the surface of mixed COOH−CH₃ SAMs and COOH content of the surface. Solid line is a theoretical fit to eq 14.

obey the Cassie equation,[68] which predicts a linear dependence on the surface composition (f_i is the surface area of component i):

$$\cos\theta = f_1\cos\theta_1 + f_2\cos\theta_2 \quad (12)$$

Agreement with the Cassie equation has also been obtained for measured contact angles on surfaces micropatterned using CH₃ and COOH groups.[69] Previous contact angles on mixed SAMs, including hydrophobic−hydrophilic components, have, however, shown substantial deviation from linearity. It was suggested[70] that in the absence of the microscopic phase segregation, surface free energies that enter eq 11 should be averaged rather than the corresponding contact angle cosines. The predicted values then agreed well with experimental trends.

Figure 7 shows that cosines of the equilibrium contact angles of epoxy polymer on mixed CH₃−COOH SAMs vary nonlinearly with the changes in the composition of the surface terminal functional groups. Since a CH₃-terminated SAM is a completely nonpolar component, eq 11 is expected to describe the data in Figure 7 with the following substitutions:

(68) Cassie, A. B. D. *Discuss. Faraday Soc.* **1948**, *3*, 11.
(69) Drelich, J.; Wilbur, J. L.; Miller, J. D.; Whitesides, G. M. *Langmuir* **1996**, *12*, 1913.
(70) Israelachvili, J. N.; Gee, M. L. *Langmuir* **1989**, *5*, 288.

$$\gamma_{CH_3-COOH}^{vW} = (1-f)\gamma_{CH_3}^{vW} + f\gamma_{COOH}^{vW} \quad (13a)$$

$$\gamma_{CH_3-COOH}^{+} = f\gamma_{COOH}^{+} \quad (13b)$$

$$\gamma_{CH_3-COOH}^{+} = f\gamma_{COOH}^{-} \quad (13c)$$

where f is the surface mole fraction (identified with surface area fraction) of the polar COOH component:

$$\cos\theta = \frac{2}{\gamma_E}[\sqrt{((1-f)\gamma_{CH_3}^{vW} + f\gamma_{COOH}^{vW})\gamma_E^{vW}} +$$

$$\sqrt{f\gamma_{COOH}^{+}\gamma_E^{-}} + \sqrt{f\gamma_{COOH}^{-}\gamma_E^{+}}] - 1$$

$$= \frac{2}{\gamma_E}\left[\sqrt{\gamma_{CH_3}^{vW}\gamma_E^{vW} + f(\gamma_{COOH}^{vW} - \gamma_{CH_3}^{vW})} +$$

$$\sqrt{f}\frac{W_{COOH/E}^{AB}}{2}\right] - 1 \quad (14)$$

Taking $\gamma_E^{vW} = 38.0$ mJ/m^2 and $\gamma_{CH_3}^{vW} = 19.3$ mJ/m^2, the trend of contact angles versus surface composition (i.e. COOH fraction) in Figure 7 is well-fitted by eqs 14 and yields $\gamma_E = 42.0 \pm 0.6$ mJ/m^2 and $\gamma_{COOH}^{vW} = 20.0 \pm 2.0$ mJ/m^2. The contribution of polar interactions to the work of adhesion between epoxy and pure COOH monolayer, $W_{COOH/E}^{AB}$, is the third fitting parameter and equals 24.1 mJ/m^2.

Considering that the surface region of the solidifying epoxy polymer is expected to rearrange in response to the varying surface composition of the SAM, the variations in the surface tension values determined with the different approaches presented above are in good agreement. Thus, $\gamma_E^{vW} = 38.0$ mJ/m^2 and $\gamma_E = 42.0$ mJ/m^2 with uncertainties on the order of 2 mJ/m^2 are the most reasonable estimates of the polymer surface free energy.

Adhesion Forces between Epoxy and Model SAM Surfaces. The results of CFM experiments to measure the work of adhesion in the epoxy-mixed SAM system are shown in Figure 8. Since contact angle data of epoxy on CH$_3$/COOH SAMs support the notion of molecular mixing in SAM, we used Ag-coated tips functionalized with mixed monolayers to systematically probe the effect of hydrogen bonding on adhesion between the polymer and SAMs supported on the tip of force microscope. From the adhesion forces found in these experiments (5−150 nN), we estimate the contact area at pull-off to be approximately 40−400 nm^2 (for $R \sim 100$ nm and $K \sim 6$ GPa, dominated by the Young's modulus for epoxy[48]), and, thus, the corresponding number of functional groups in the contact zone is 200−2000 (with 0.2 nm^2/group).[30] Therefore, even for this microscopic type of measurement one can assume that the actual SAMs composition on the tip is representative of the average surface composition determined spectroscopically.

The thermodynamic work of adhesion of solid epoxy polymer with a tip-supported SAM in water, W_{EWS}, is expressed by the balance of interfacial free energies (epoxy−water (EW); SAM−water (SW), and epoxy−SAM (ES)):

$$W_{EWS} = \gamma_{EW} + \gamma_{SW} - \gamma_{ES} = \gamma_E \cos\theta_{ES} -$$

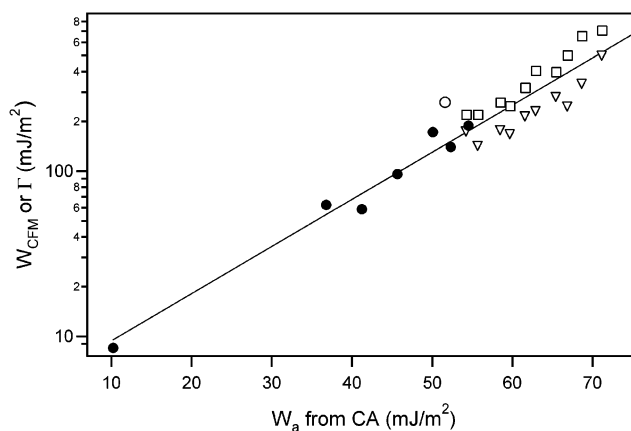$$\gamma_W \cos\theta_{WS} + \gamma_{EW} \quad (15)$$

Figure 8. Work of adhesion between AFM tips terminated in mixed COOH−CH$_3$ SAMs and epoxy samples estimated from CFM measurements in water (●) and air (○) and polymer strip pull-off tests in air[48] (open symbols, □ and ▽, designate data for polymer strips of different widths, 20 and 40 μm, respectively) as a function of thermodynamic work of adhesion, W_a, determined from contact angle data as discussed in the text.
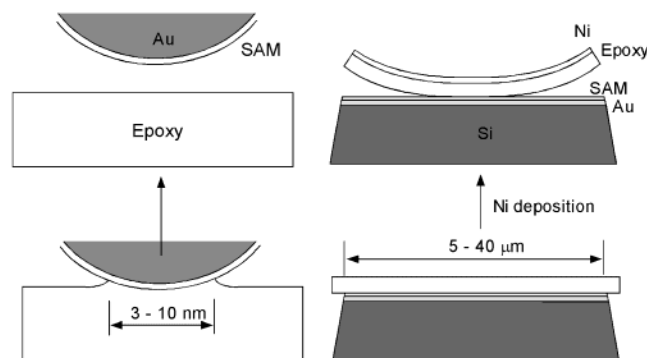

Figure 9. Configuration of the "pull-off" experiments in the CFM and superlayer tests for measurements of interfacial fracture energy (note 3 orders of magnitude difference in scale).

where in the second equality Young's equation is used ($\gamma_i \cos\theta_{iS} = \gamma_S - \gamma_{iS}$, $i = $ W or E). The last quantity in eq 15 is independent of the SAM composition and can be calculated to be ~20 mJ/m^2 with the aid of the surface tension component theory using reported values for water and values for epoxy determined above. Using eq 11, one can obtain the corresponding values of W_{ES} in ambient conditions. The two values W_{ES} and W_{EWS}, calculated with the experimental values of θ_{ES} and θ_{WS}, display two diverging trends: work of adhesion in air increases for COOH rich SAMs, whereas higher COOH fraction in SAM leads to lower values for work of adhesion in water.

In addition to CFM, a "superlayer test" was used to measure interfacial fracture energy between micromolded epoxy strips and mixed self-assembled monolayers.[48] The CFM and superlayer test configurations are compared in Figure 9. There appears to be a general correlation between the work of adhesion determined from contact angles and values found in "pull-off" experiments at micro- and nanoscale for the epoxy−SAM system. This correlation is evident in the plot of the work of adhesion from CFM (determined in water) and fracture energies from superlayer tests (in air)[48] versus the thermodynamic work of adhesion calculated from contact angles data (Figure 8). The general trend is the same as one observed for model monolayer systems: an increase in the hydrogen bonding character of the SAM surface substantially reduces the adhesion between the polar polymer and the SAM surface in water. The opposite is
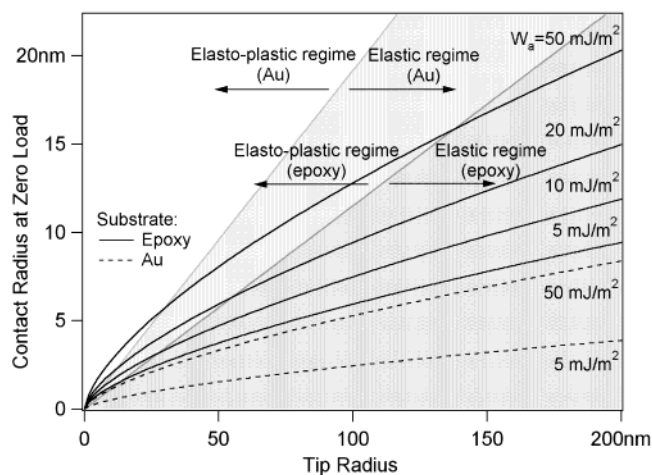
Figure 10. Contact radius for the onset of inelastic deformations[71] (boundaries of shaded areas) on gold (Young's modulus $E = 78$ GPa, yield strength $Y = 6$ GPa) and epoxy ($E = 3$ GPa, $Y = 150$ MPa) samples and contact radius at zero applied load (solid and dashed lines) for different values of the work of adhesion, W_a, versus probe radius. Note that intrinsic yield strength of Au nanocontacts[72] was used rather than the bulk value.

true for adhesion in air: the work of adhesion increases as the monolayer is enriched with a hydrogen bonding component. Unlike the SAM–SAM interactions, there is a substantial inelastic contribution to epoxy–SAM adhesion measured in force experiments. The slope of the curve in the Figure 8 quickly deviates from one for high values of thermodynamic work of adhesion determined from contact angle measurements. For superlayer tests, connections between fracture energies, the surface energies, and the inelastic deformations occurring in the epoxy have been extensively explored.

JKR analysis extended by Maugis and Pollock[71] to include plastic deformations indeed predicts different behavior for the SAM–SAM and SAM–epoxy systems in the CFM measurements. Figure 10 compares contact radius at zero load given by the JKR theory to the contact radius at the onset of inelastic deformation for a range of probe radii. While for SAMs on Au the CFM experiments remain in the elastic regime for the full range of W_a, the tip induced deformations of the epoxy substrate enter the elastoplastic regime at higher values of W_a. Typically, when the deformation at zero load begins on the tip axis, the plastic zone at the edge of the contact area is already well-developed[71] and will contribute to the measured pull-off forces.

(71) Maugis, D.; Pollock, H. M. *Acta Metall.* **1984**, *32*, 1323.
(72) Stalder, A.; Durig, U. *J. Vac. Sci. Technol. B* **1996**, *14*, 1259.

For this polymer, increase in W_a by a factor of 5 leads to an increase in the measured (JKR) work of adhesion by a factor of 20.

Conclusions

Chemical force microscopy was used to study chemical and solvent effects on adhesive interactions using SAMs as model systems. The more complex interactions between a synthetic epoxy polymer and SAMs were also examined. We found that the chemical composition of the SAM on the tip and chemical composition of the SAM on the substrate surfaces and nature of the of the medium all contributed heavily to adhesion. Complementary extensive macroscopic contact angle measurements were used to assist in the quantitative interpretation of the CFM results. This self-consistent data set was used to demonstrate that it is important to account accurately for the balance of hydrogen bonding interactions in quantitative interpretations of direct adhesion force measurements between organic surfaces in liquids. The hydrogen bonding properties of both the solvent and interacting surfaces have a profound effect on measured forces. Adhesion between surfaces of polar epoxy polymer and model monolayers of varying hydrogen bonding ability correlates with the SAM composition. Van der Waals type interactions alone are not sufficient to explain observed trends. Semiempirical treatments, for example the FOCG theory of the intermolecular forces, are useful in rationalizing the force microscopy results.

This study is an attempt to apply the methodology of chemical force microscopy to more complex systems such as polymers and to develop a framework for interpreting adhesion force measurements in a liquid medium with this technique. We have shown that CFM experiments were useful in understanding the nature of intermolecular forces determining adhesion measured macroscopically. The relevant work of adhesion then can be unambiguously determined. The degree of hydrogen bonding of the probe for CFM of polymers can be efficiently controlled with a composition of a mixed SAM. The possibility of an inelastic contribution to the work of adhesion should always be assessed for CFM measurements involving polymer surfaces. As instrument and probe calibration improves and tip modification becomes more standard, we expect these types of studies to be a valuable complement to existing macroscopic methods.

JA025951M